THE JOURNAL OF PHYSICAL CHEMISTRY B

ARTICLE

pubs.acs.org/JPCB

Temperature Dependence of Ion Transport in Dilute Tetrabutylammonium Triflate-Acetate Solutions and Self-Diffusion in Pure Acetate Liquids

Dharshani N. Bopege,[†] Matt Petrowsky,[‡] Allison M. Fleshman,[‡] Roger Frech,*[,‡] and Matthew B. Johnson[†]

[†]Homer L. Dodge Department of Physics and Astronomy, University of Oklahoma, 440 West Brooks Street, Norman, Oklahoma 73019, United States

[‡]Department of Chemistry and Biochemistry, University of Oklahoma, 101 Stephenson Parkway, Norman, Oklahoma 73019, United States

ABSTRACT: Conductivities and static dielectric constants for 0.0055 M tetrabutylammonium trifluoromethanesulfonate in *n*-butyl acetate, *n*-pentyl acetate, *n*-hexyl acetate, *n*-octyl acetate, and *n*-decyl acetate have been collected over the temperature range of 0−80 °C. Self-diffusion coefficients and static dielectric constants of pure acetates were obtained over the same temperature range. Both temperature-dependent diffusion coefficients and ionic conductivities of these pure acetates and dilute acetate solutions can be accurately described by the compensated Arrhenius formalism. Activation energies were calculated from compensated Arrhenius plots for both conductivity and diffusion data. Activation energies are higher for conductivity data of 0.0055 M TbaTf-acetates compared to diffusion data of pure acetates. The plot of the exponential prefactor versus the dielectric constant yields a single master curve for both conductivity and diffusion data. These data support the argument that mass and charge transport are thermally activated processes in the acetates, as previously observed in alcohol-based electrolytes.

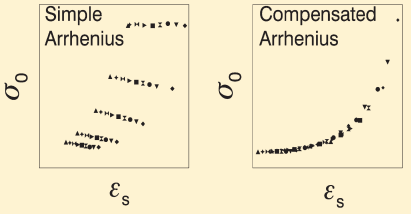

INTRODUCTION

It is important to understand charge and mass transport in organic liquid electrolytes and polymer electrolytes (PEs) due to their importance in applications such as lithium rechargeable batteries and other electrochemical devices.[1−4] The temperature dependence of ionic conductivity and diffusion in these electrolytes can provide information about complex system dynamics. The simple Arrhenius equation shown in eq 1 describes the temperature dependence of ionic conductivity below the glass transition temperature, T_g, for PEs.[5−8]

$$\sigma = \sigma_0 e^{-E_a/RT} \quad (1)$$

Here, σ denotes the ionic conductivity, σ_0 is the temperature-independent prefactor, T is the temperature, and E_a is the activation energy. It has been found that liquid electrolytes and PEs above T_g often show non-Arrhenius conductivity behavior that is commonly described using the Vogel−Tammann−Fulcher (VTF) or the Williams−Landel−Ferry (WLF) empirical equations.[9−12] However, the resulting fitting parameters of these equations do not provide an explanation for the underlying mechanism of ion transport.

Recently, a new approach has been proposed to describe charge and mass transport in pure liquids and liquid electrolytes.[13−16] The temperature-dependent conductivity is formally written as an Arrhenius-like expression; however, in contrast to eq 1, there exists a temperature dependence in the exponential prefactor that is due to the temperature dependence of the solvent/solution static dielectric constant (ε_s). Therefore, the ionic conductivity can be written as

$$\sigma(T, \varepsilon_s) = \sigma_0(\varepsilon_s(T))e^{-E_a/RT} \quad (2)$$

This dielectric constant dependence in the prefactor is removed by using a scaling procedure that has been previously described in detail.[13−16] The scaling procedure requires a reference curve. A reference conductivity curve is constructed from the isothermal conductivity and static dielectric constant values of each member of a solvent family. Here, the family members are *n*-butyl, *n*-pentyl, *n*-hexyl, *n*-octyl, and *n*-decyl acetate. The temperature at which each reference conductivity is measured is termed the reference temperature, T_r. The end result of this scaling procedure is the compensated Arrhenius equation (CAE), given as eq 3

$$\ln\left[\frac{\sigma(T, \varepsilon_s)}{\sigma(T_r, \varepsilon_s)}\right] = \frac{-E_a}{RT} + \frac{E_a}{RT_r} \quad (3)$$

If CAE behavior is observed, a plot of $\ln(\sigma(T,\varepsilon_s)/\sigma_r(T_r,\varepsilon_s))$ versus $1/T$ yields a straight line with slope $-E_a/R$ and intercept $E_a/(RT_r)$. The activation energy can be calculated from either the slope or the intercept of eq 3. The agreement between these two activation energies provides a measure of the validity of this procedure. This activation energy is used to determine the exponential prefactor, σ_0, by dividing $\sigma(T,\varepsilon_s)$ by the Boltzmann factor ($\exp[-(E_a/RT)]$). Previous work has shown that a master curve results when the prefactors are plotted against the dielectric constant.[13−16] The formation of a master curve supports the postulates underlying eq 2. The compensated Arrhenius formalism (CAF) has been used to describe self-diffusion and dielectric relaxation transport phenomena in addition to ionic conductivity.[13,16]

Received: September 9, 2011
Revised: November 2, 2011
Published: December 06, 2011

The self-diffusion coefficients (D) can be presented in the following form analogous to eq 2.

$$D(T, \varepsilon_s) = D_0(\varepsilon_s(T))e^{-E_a/RT} \quad (4)$$

Here, $D_0(\varepsilon_s(T))$ is the exponential prefactor.

Translational diffusion data complement ionic conductivity data in studies of transport in an electrolyte. Pulsed field gradient nuclear magnetic resonance (PFG-NMR) spectroscopy is a powerful tool for determining diffusion coefficients and is used in this work and related studies.[17−26] It has been shown that temperature-dependent diffusion coefficients exhibit the same compensated Arrhenius behavior as ionic conductivities.[13] The temperature dependence of both ionic conductivities and self-diffusion coefficients for alcohol-based electrolytes and pure alcohols, respectively, have been studied using the CAF.[13,14] Similar studies must be performed for other solvent systems in order to test the generality of this approach.

In this study, the temperature dependence is examined for ionic conductivities of 0.0055 M TbaTf-acetate solutions as well as self-diffusion coefficients of pure acetates. In the conductivity studies, tetrabutylammonium trifluoromethanesulfonate (TbaTf) was chosen as the solute because it minimizes the cation−anion interactions in solution. The bulky butyl groups prevent contact ionic association, and therefore, only "free" ions exist in solution.[27,28] The IR spectrum of TbaTf-butyl acetate (0.2 m) has only one band at 753 cm^{-1} in the CF_3 symmetric deformation region of the triflate ion, which is indicative of unperturbed triflate ions. This observation supports the claim that there are no discrete, ionically associated species even in these very low permittivity TbaTf-acetate solutions. The main objective of this work is to verify the CAF using pure acetates and dilute acetate-based electrolytes.

EXPERIMENTAL SECTION

Sample Preparation. All acetates and TbaTf were purchased from either Aldrich or Alfa Aesar and used as received. All materials were stored and electrolyte solutions prepared in a drybox under a nitrogen atmosphere (≤1 ppm H_2O and approximate temperature of 25 °C). A 0.0055 M (molar concentration, mol/L) sample was made by dissolving an appropriate amount of TbaTf into a particular acetate solvent, followed by stirring for 24 h.

Conductivity and Static Dielectric Constant measurements. For the conductivity and dielectric constant measurements, the TbaTf-acetate solution or pure acetate solvent was contained in a liquid cell (Agilent 16452A with a 2 mm spacer) immersed in an oil bath.[29] All measurements were carried out over a temperature range from 0 to 80 °C using a Huber ministat 125 with an accuracy of ±0.1 °C. The capacitance and conductance were measured at each temperature with an impedance analyzer (HP 4192A scanning the frequency range of 1 kHz to 13 MHz). The measured conductance, in conjunction with the known cell geometry, was used to determine the solution conductivity at each temperature. The solution and pure solvent static dielectric constants were calculated using the relation $\varepsilon_s = \alpha C/C_0$, where C is the sample capacitance and C_0 is the atmospheric capacitance. The parameter α, which is close to unity, accounts for stray capacitance.[29]

PFG NMR Self-Diffusion Measurements. A NMR capillary tube (5 mm OD and 20 cm long) was filled to a 0.8 cm height with pure acetate solvent for the NMR-PFG measurements. This tube was sealed with parafilm after filling the sample in a drybox (≤1 ppm H_2O). PFG measurements were performed using a Varian VNMRS 400 MHz NMR spectrometer, which was operated with an Auto-X-Dual broad-band 5 mm probe tuned to 399.870 MHz for protons. The standard Stejskal−Tanner pulsed gradient sequence was performed at each temperature (from 0 to 80 °C) by arraying the gradient field strength from 6 to 62 G/cm.[20,30−32] The integrated intensity of each attenuated signal was calculated. The diffusion coefficient was calculated from the slope of the plot of ln(intensity) versus the square of the gradient strength. The temperature was controlled using an FTS XR401 air-jet regulator. The duration of the gradient pulse encompassed the range from 0.27 (butyl acetate at 70 °C) to 1.7 ms (decyl acetate at 0 °C).

RESULTS AND DISCUSSION

Temperature Dependence of Ion Transport in 0.0055 M TbaTf-Acetates. The ionic conductivities and solution dielectric constants of 0.0055 M TbaTf-acetate solutions were calculated from the measured conductance and capacitance data, respectively. Electrode polarization produces artificially high capacitance measurements at lower frequencies, but this effect decreases as the frequency increases. At higher frequencies, a plateau region for the capacitance was observed between 10^4 and 10^7 Hz for each acetate solution. The value of the real part of the dielectric constant calculated from this plateau capacitance is designated as ε_s and here denotes the static dielectric constant. As mentioned earlier, choosing a reference conductivity curve is very important for the scaling procedure. In this study, reference curves were constructed for six different reference temperatures (20, 30, 40, 50, 60, and 80 °C). Each reference curve includes butyl, pentyl, hexyl, octyl, and decyl acetate and was fitted using the empirical function $\sigma = A \times \exp(\varepsilon_s/t) + B$ (ExpGro1 in OriginLab Origin 8.1 software). Here, A, B, and t are the fitting parameters.

Figure 1 presents a comparison of the simple Arrhenius plot and compensated Arrhenius plot for 0.0055 M TbaTf in hexyl acetate from 0 to 80 °C. The left and right y axes denote scaled temperature-dependent ionic conductivities (CAE) and conductivity values for the simple Arrhenius equation, respectively. The compensated Arrhenius plot was prepared using a reference temperature, T_r = 40 °C. Both plots show linear behavior and have correlation coefficients close to unity.

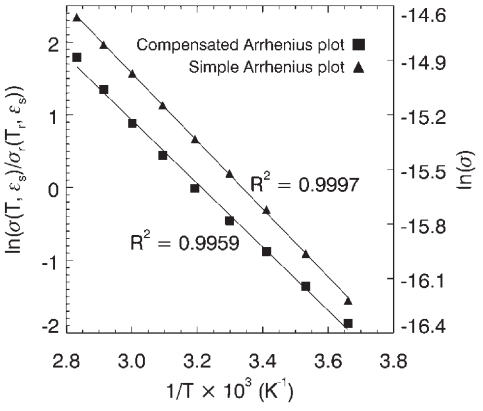

Figure 1. Simple Arrhenius and compensated Arrhenius plots for conductivity data of 0.0055 M TbaTf-hexyl acetate.

dx.doi.org/10.1021/jp208742h |J. Phys. Chem. B 2012, 116, 71–76

Table 1. Activation Energies from Compensated Arrhenius and Simple Arrhenius Plots Resulting from Conductivity Data for 0.0055 M TbaTf-Acetates

		CAE E_a (kJ mol^{-1})		simple Arrhenius E_a (kJ mol^{-1})	
0.0055 M TbaTf solvent	T_r (°C)	slope	intercept	0.0055 M TbaTf solvent	slope
pentyl acetate	20	36.3 ± 0.8	36.3 ± 0.8	butyl acetate	11.3 ± 0.1
	30	35.7 ± 0.8	35.8 ± 0.8	pentyl acetate	13.1 ± 0.1
	40	35.7 ± 0.8	35.9 ± 0.8	hexyl acetate	15.5 ± 0.1
hexyl acetate	20	36.1 ± 0.9	36.1 ± 0.8	octyl acetate	19.4 ± 0.1
	30	38 ± 1	38 ± 1	decyl acetate	28 ± 1.0
	40	36.3 ± 0.9	36.5 ± 0.9		
	50	35.9 ± 0.7	36.0 ± 0.7		
	60	36.4 ± 0.7	36.5 ± 0.7		
octyl acetate	60	39.2 ± 0.9	39 ± 1		
	80	35.8 ± 0.9	35 ± 1		

However, very different E_a values result from the CAF analysis compared to the simple Arrhenius analysis. For example, the activation energy calculated from the conductivity data for 0.0055 M TbaTf-hexyl acetate using the simple Arrhenius plot is 15.5 ± 0.1 kJ mol^{-1}, while the compensated Arrhenius plot yields a value of 36.4 ± 0.9 kJ mol^{-1} at T_r = 40 °C. This difference results from the significant disparity in the two slopes, noting the distinction in scale in the two ordinate axes. Table 1 shows E_a values from CAE plots that result from the conductivity data of 0.0055 M TbaTf-acetates and also E_a values from the simple Arrhenius plots of these data. The CAE E_a values in Table 1 are closely grouped when an appropriate reference temperature is chosen for each acetate member. The reference temperature is chosen such that the temperature-dependent dielectric constant range of the family member is encompassed by the dielectric constant range of the reference conductivity curve.[15]

The average activation energy calculated from the CAF is 36.5 ± 0.8 kJ mol^{-1}, while E_a values resulting from simple Arrhenius plots increase systematically with acetate chain length. Simple Arrhenius behavior is observed over the entire temperature range in each acetate member except decyl acetate, which is the longest-chain member studied and has very low conductivities. The conductivity data collected at subambient temperatures for decyl acetate are close to the detection limit of the impedance analyzer and were therefore omitted from the analysis.

Figure 2 plots the conductivity versus static dielectric constant for 0.0055 M TbaTf-acetate solutions over the temperature range from 0 to 80 °C. Five distinct curves are observed, each one consisting of the temperature-dependent data for a particular acetate member. These data comprise a series of isothermal reference curves. For example, if a reference temperature of 40 °C was selected, the five data points designated by the solid squares would form the reference curve at 40 °C.

The exponential prefactor is obtained by dividing the temperature-dependent conductivity by $\exp(-E_a/RT)$. Figure 3 graphs the exponential prefactor against the dielectric constant for two different E_a values. All data points lie on a single curve, as shown in Figure 3a, when the CAE average E_a value is used. A master curve is still observed when arbitrarily choosing an E_a value in the range from 32 to 42 kJ mol^{-1}. It is interesting to note that the median value of this range (37 kJ mol^{-1}) is close to the average E_a (36.5 kJ mol^{-1}).

Figure 3b was plotted using E_a = 11.3 ± 0.1 kJ mol^{-1} obtained from the simple Arrhenius plot of butyl acetate. It is evident that

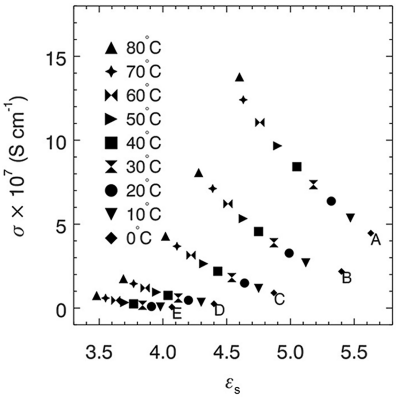

Figure 2. Conductivity versus static dielectric constant for 0.0055 M TbaTf-acetate solutions of (A) butyl acetate, (B) pentyl acetate, (C) hexyl acetate, (D) octyl acetate, and (E) decyl acetate over the temperature range of 0−80 °C.

the data do not form a single master curve. According to these results, the qualitative shape of the graph varies significantly depending on the E_a value, thus supporting the necessity of the compensation procedure to obtain a meaningful value of the activation energy.

Temperature Dependence of Self-Diffusion Coefficients for Pure Acetate Solvents. In this section, the CAF is used to analyze the self-diffusion coefficients measured with PFG-NMR for pure *n*-butyl, *n*-pentyl, *n*-hexyl, *n*-octyl, and *n*-decyl acetates over the temperature range of 0−80 °C. Energy of activation values were calculated using a procedure similar to that for temperature-dependent conductivity data. Linear behavior is observed for both simple Arrhenius and compensated Arrhenius plots, as shown in Figure 4 for pure octyl acetate. The E_a value calculated from a simple Arrhenius plot is substantially different from that found from a compensated Arrhenius plot, as was observed with the conductivity data. On the basis of the compensated Arrhenius plots for hexyl and octyl acetate at five reference temperatures (20, 30, 40, 50, and 60 °C), an average activation energy of 25.5 ± 0.9 kJ mol^{-1} is obtained. Table 2 summarizes E_a values calculated from the CAE slope and intercept for two pure acetates. Table 2 also reports activation energies obtained from simple Arrhenius plots.

dx.doi.org/10.1021/jp208742h | J. Phys. Chem. B 2012, 116, 71–76

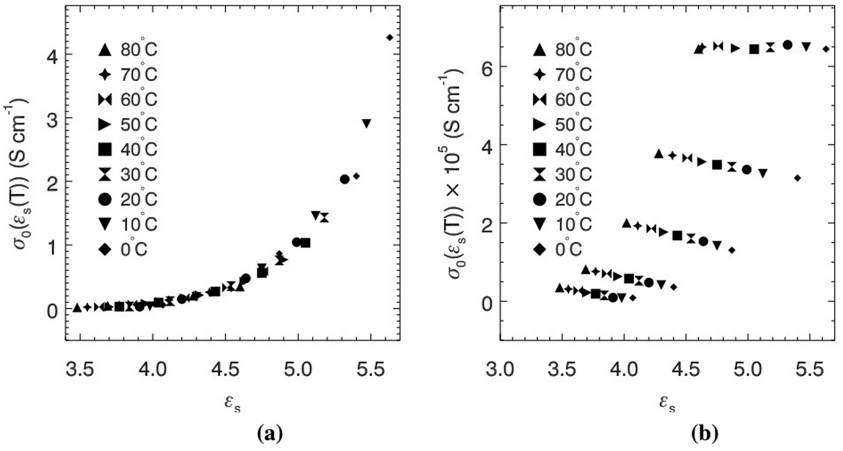

Figure 3. Conductivity exponential prefactor versus dielectric constant for 0.0055 M TbaTf-acetate solutions using (a) E_a = 36.5 and (b) 11.3 kJ mol^{-1}.

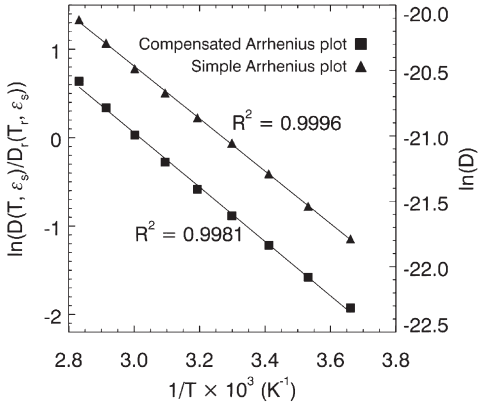

Figure 4. Simple Arrhenius and compensated Arrhenius (at T_r = 60 °C) plots from diffusion data for pure octyl acetate.

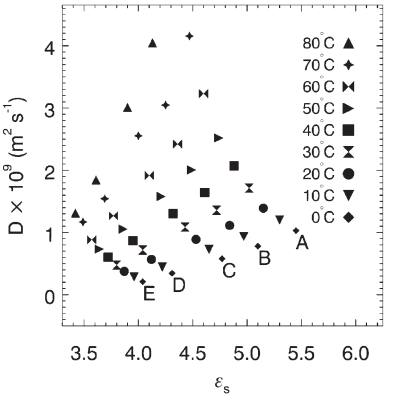

Figure 5. Self-diffusion coefficients versus static dielectric constant for (A) butyl acetate, (B) pentyl acetate, (C) hexyl acetate, (D) octyl acetate, and (E) decyl acetate.

Table 2. Activation Energies from Compensated and Simple Arrhenius Plots Resulting from Diffusion Data for Pure Acetates

		CAE E_a (kJ mol^{-1})		simple Arrhenius E_a (kJ mol^{-1})	
solvent	T_r (°C)	slope	intercept	solvent	slope
hexyl acetate	20	26 ± 1	26 ± 1	butyl acetate	15 ± 1
	30	25 ± 1	26 ± 1	pentyl acetate	16.0 ± 0.8
	40	25 ± 1	25 ± 1	hexyl acetate	16.4 ± 0.6
	50	26 ± 1	26 ± 1	octyl acetate	16.7 ± 0.1
octyl acetate	50	24.9 ± 0.5	25.0 ± 0.5	decyl acetate	18.4 ± 0.3
	60	25.6 ± 0.4	25.7 ± 0.4		

Figure 5 plots temperature-dependent self-diffusion coefficients versus dielectric constants for the family of pure acetates. The temperature-dependent diffusion coefficients for each member lie on well-separated curves, similar to the conductivity data depicted in Figure 2.

The exponential prefactor, $D_0(\varepsilon_s(T))$, can be determined by dividing the diffusion coefficient by the Boltzmann factor according to eq 4. Figure 6a plots the exponential prefactor versus dielectric constant for pure acetates using the average CAE E_a value, while Figure 6b presents this data using the E_a value obtained from the simple Arrhenius plot for hexyl acetate. Similar to the conductivity data, a master curve is not observed for E_a values obtained from a simple Arrhenius plot. A master curve does result for E_a values within the narrow range from 24 to 27 kJ mol^{-1}. The average activation energy from the CAF analysis is equal to the median value of this range. The diffusion master curve exhibits more scatter in the data than the analogous plot for conductivity. It is likely that at least some of the scatter is due to convection effects. Pronounced thermal gradients can exist in the NMR sample when the sample temperature significantly deviates from room temperature. These thermal gradients produce artificially high values for the diffusion coefficients. Convection-related error was minimized in this study by focusing on the longer chain acetates that are less susceptible to this phenomenon and also by constricting the sample volume in the NMR tube. However, it is difficult to completely eliminate convection effects, and consequently, some error is introduced into the diffusion data at higher temperatures.

CONCLUSIONS

In this study, we extend the scope of the CAF by examining the family of *n*-acetates, which are aprotic, very low dielectric

dx.doi.org/10.1021/jp208742h |*J. Phys. Chem. B* 2012, 116, 71–76

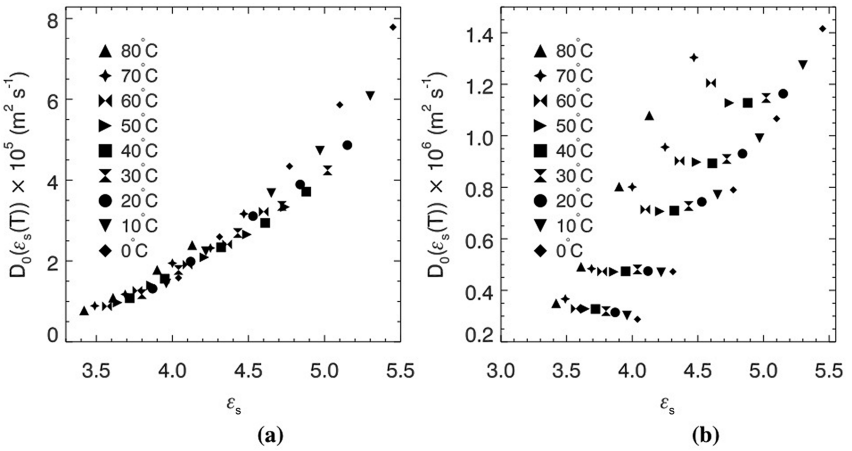

Figure 6. Exponential prefactor versus dielectric constant for the diffusion data of pure acetates using (a) E_a = 25.5 and (b) 16.4 kJ mol^{-1}.

constant solvents. Here, temperature-dependent conductivities and self-diffusion coefficients are reported for 0.0055 M TbaTf-acetate electrolytes and pure acetates, respectively. Our results indicate that both temperature-dependent ionic conductivity and diffusion coefficient data for acetates obey the compensated Arrhenius formalism. The reported activation energy from diffusion data of pure acetates is 25.5 kJ mol^{-1}, while that obtained from conductivity data for 0.0055 M TbaTf-acetates is 36.5 kJ mol^{-1}. The difference between these two activation energies (approximately 11 kJ mol^{-1}) is significant. Ketones are structurally very similar to the acetates but have much higher dielectric constants. Studies are currently underway to examine diffusion and conductivity in pure ketones and dilute ketone electrolytes. A comparison between acetate and ketone conductivity and diffusion data is necessary to better understand the role of the static dielectric constant in controlling mass and charge transport in liquids.

The conductivity and diffusion data presented here for butyl, pentyl, hexyl, octyl, and decyl acetate are described very well with the CAF. However, acetates with shorter alkyl chains were not included in the analysis because their transport behavior is not entirely consistent with that for the long-chain acetates. Figure 7 plots the conductivity versus the dielectric constant for 0.0055 M TbaTf-acetates. This graph is similar to Figure 2 except that data are included for methyl, ethyl, and propyl acetate. The conductivities for the three shortest-chain members are much higher than those for the longer members. If data for methyl, ethyl, and propyl acetate are included in the reference curve, the conductivity CAE plots for ethyl and propyl acetate result in E_a values around 28 kJ mol^{-1}. This activation energy is well below the average E_a value calculated for the longer members (36.5 kJ mol^{-1}). Furthermore, CAE plots for each of the longer members give E_a values that are close to the average value of 36.5 kJ mol^{-1} (see Table 1). The CAF can only completely describe the acetate data if this family is subdivided into two groups that have different E_a values. The lower activation energy for methyl, ethyl, and propyl acetate helps explain the high conductivity values observed for these members in Figure 7. Additionally, the conductivity prefactors for methyl, ethyl, and propyl acetate show the same dielectric constant dependence as that for the long-chain acetates in Figure 3a, except that these data are slightly offset to the right of the master curve.

Methyl, ethyl, and propyl acetate are not the only short-chain members of a solvent family to show deviations from the CAF. Both dielectric relaxation data for acetonitrile[16] and diffusion data for

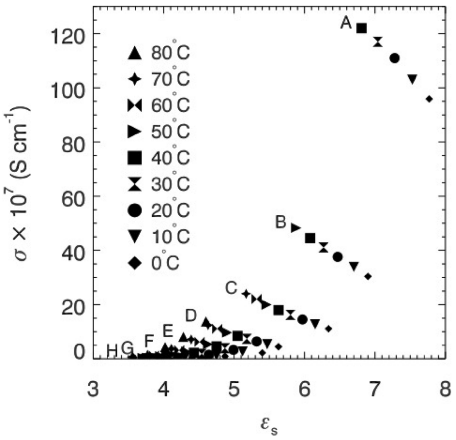

Figure 7. Conductivity versus static dielectric constant for 0.0055 M TbaTf-acetate solutions of (A) methyl acetate, (B) ethyl acetate, (C) propyl acetate, (D) butyl acetate, (E) pentyl acetate, (F) hexyl acetate, (G) octyl acetate, and (H) decyl acetate over the temperature range of 0−80 °C.

methanol[13] have been shown to exhibit transport behavior that is different from that of their long-chain family members. Previous work has shown that the CAF can be applied to dielectric relaxation data for pure acetates.[16] However, data for methyl and propyl acetate were included in the previous calculation of the activation energy. Therefore, it is possible that the reported E_a value is somewhat different from an activation energy calculated using only long-chain acetates.

AUTHOR INFORMATION

Corresponding Author

*E-mail: rfrech@ou.edu. Phone: +1 (405)325 3831. Fax: +1 (405)325 6111.

ACKNOWLEDGMENT

We wish to thank the Army Research Office for their support of this research (Grant W911NF-10-1-0437). We would like to thank Dr. Susan Nimmo for her guidance with the NMR diffusion measurements. We also thank the National Science Foundation for its financial support of the NMR equipment (Grant

CHE#0639199). We are grateful to Chris Crowe who created the labview program that automated the impedance analyzer. We are thankful to Jeremy D. Jernigen and R. S. P. Bokalawela for their support.

REFERENCES

(1) Fauteux, D.; Massucco, A.; McLin, M.; Buren, M. V.; Shi, J. *Electrochim. Acta* **1995**, *40*, 2185–2190.
(2) Xu, K. *Chem. Rev.* **2004**, *104*, 4303–4417.
(3) MacCallum, J. R.; Vincent, C. A. *Polymer electrolyte reviews 1*, 1st ed.; Elsevier Applied Science Publishers Ltd.: New York, 1987.
(4) MacCallum, J. R.; Vincent, C. A. *Polymer electrolyte reviews 2*, 1st ed.; Elsevier Applied Science Publishers Ltd.: New York, 1989.
(5) Bendler, J.; Fontanella, J. J.; Shlesinger, M. F. *Phys. Rev. Lett.* **2001**, *87*, 195503.
(6) Arrhenius, S. *Z. Phys. Chem.* **1889**, *4*, 226.
(7) Fontanella, J.; Wintersgill, M.; Smith, M.; Semancik, J.; Andeen, C. *J. Appl. Phys.* **1986**, *60*, 2665–2671.
(8) Bruce, P. G. *Solid State Electrochemistry*, 1st ed.; Cambridge University Press: New York, 1995.
(9) Williams, M. L.; Landel, R. F.; Ferry, J. D. *J. Am. Chem. Soc.* **1955**, *77*, 3701–3707.
(10) Vogel, H. *Physik Z.* **1921**, *22*, 645–646.
(11) Fulcher, G. S. *J. Am. Ceram. Soc.* **1925**, *8*, 339–355.
(12) Tammann, G.; Hesse, W. *Z. Anorg. Allg. Chem.* **1926**, *156*, 245–257.
(13) Petrowsky, M.; Frech, R. *J. Phys. Chem. B* **2010**, *114*, 8600–8605.
(14) Petrowsky, M.; Frech, R. *J. Phys. Chem. B* **2009**, *113*, 5996–6000.
(15) Fleshman, A. M.; Petrowsky, M.; Jernigen, J. D.; Bokalawela, R. S. P.; Johnson, M. B.; Frech, R. *Electrochim. Acta* **2011**, *57*, 147–152.
(16) Petrowsky, M.; Frech, R. *J. Phys. Chem. B* **2009**, *113*, 16118–16123.
(17) Williamson, M. J.; Hubbard, H. V. S. A.; Ward, I. M. *Polymer* **1999**, *40*, 7177–7185.
(18) Boden, N.; Leng, S.; Ward, I. *Solid State Ionics* **1991**, *45*, 261–270.
(19) Williamson, M.; Southall, J.; Hubbard, H. S. A.; Johnston, S.; Davies, G.; Ward, I. *Electrochim. Acta* **1998**, *43*, 1415–1420.
(20) Zhu, X. X.; Macdonald, P. M. *Macromolecules* **1992**, *25*, 4345–4351.
(21) Hayamizu, K.; Aihara, Y.; Arai, S.; Martinez, G. *J. Phys. Chem. B* **1999**, *103*, 519–524.
(22) Johansson, A.; Gogoll, A.; Tegenfeldt, J. *Polymer* **1996**, *37*, 1387–1393.
(23) Aihara, Y.; Bando, T.; Nakagawa, H.; Yoshida, H.; Hayamizu, K.; Akiba, E.; Price, W. S. *J. Electrochem. Soc.* **2004**, *151*, A119–A122.
(24) Hayamizu, K.; Matsuo, A.; Arai, J. *J. Electrochem. Soc.* **2009**, *156*, A744–A750.
(25) Holz, M.; Heil, S. R.; Sacco, A. *Phys. Chem. Chem. Phys.* **2000**, *2*, 4740–4742.
(26) Ferry, A.; Orädd, G.; Jacobsson, P. *Electrochim. Acta* **1998**, *43*, 1471–1476.
(27) Frech, R.; Huang, W. *J. Solution Chem.* **1994**, *23*, 469–481.
(28) Petrowsky, M.; Frech, R. *J. Phys. Chem. B* **2008**, *112*, 8285–8290.
(29) *Agilent 16452A Liquid Test Fixture Operation and Service Manual*; 2000.
(30) Stejskal, E. O.; Tanner, J. *J. Chem. Phys.* **1965**, *42*, 288–292.
(31) Price, W. S. *Concepts Magn. Reson.* **1997**, *9*, 299–336.
(32) Price, W. S. *Concepts Magn. Reson.* **1998**, *10*, 197–237.